APPLICATIONS OF MOLECULAR SPECTROSCOPY METHODS TO THE STUDY OF METAL DUSTING CORROSION*

V.A. Maroni
Chemical Technology Division
Argonne National Laboratory
9700 South Cass Ave.
Argonne, IL 60439

February 2002

Paper prepared for publication in the
Proceedings of the International Workshop on Metal Dusting
September 26-28, 2001
Argonne National Laboratory, Argonne, IL

*****This research was sponsored by the Office of Industrial Technologies, U.S. Department of Energy under Contract W-31-109-ENG-38.

APPLICATIONS OF MOLECULAR SPECTROSCOPY METHODS TO THE STUDY OF METAL DUSTING CORROSION

V.A. MARONI, Argonne National Laboratory, Argonne, Illinois*

ABSTRACT

The interrogation of molecular vibrations in crystalline and amorphous solids by Raman and infrared spectroscopy methods can provide a wealth of revealing information concerning the composition, morphology, and spatial distribution of the extant phases. When these measurements are made in situ, such as during processes taking place in extreme environments (e.g., elevated temperature and pressure, oxidizing or reducing), where phases are evolving and/or dissipating, it is also possible to derive kinetic and mechanistic parameters. This paper summarizes the possibilities and limitations involved in using various types of Raman and infrared measurement methods to study metal dusting corrosion. Applications of conventional, microprobe, and imaging molecular spectroscopy approaches are discussed, with examples taken directly from metal dusting investigations. Some perspective is offered concerning the origin of observable condensed matter phonons emanating from the surface films and the carbon particles that accompany carbon dusting on various types of metals and alloys. Concepts for the systematic investigation of carbon dusting chemistry using molecular spectroscopy methods are presented.

INTRODUCTION

The application of molecular spectroscopy methods to problems in materials science is receiving increased emphasis. The molecular vibrations or, in the case of solid materials, the phonons that are detectable by molecular spectroscopy measurement techniques are characteristic/indicatory features of molecular and crystalline materials. Since the issues involved in the examination of carbon dusting corrosion deal primarily with solid phases, the remainder of the discussion will summarily describe the measurement and interpretation of the molecular spectra of solids, using examples taken from Raman studies of the carbon dusting corrosion of iron.

The most commonly used methods for measuring molecular spectra are based on Raman scattering and on the absorption, transmission, or reflection of infrared radiation. Laser-excited Raman spectroscopy, dispersive infrared spectroscopy, and Fourier transform infrared (FTIR) spectroscopy are well-developed methods and the associated instrumentation can be found in virtually all laboratories where comprehensive materials analyses are performed. Informative discussions of the general methodologies and their application to solid materials can be found, e.g., in Suëtaka (1995) and Ferraro and Krishnan (1990). Two features of the Raman and infrared instrumentation methodologies that make them especially useful for the study of corrosion processes and corroded specimens are (1) their adaptability to in situ investigations (including conditions of elevated temperature and wide ranging pressure) and (2) the effective use that can be made of their integration with conventional optical and confocal microscopes.

* *Corresponding author address:* Victor A. Maroni, Argonne National Laboratory, 9700 South Cass Ave., Argonne, IL 60439; e-mail: Maroni@cmt.anl.gov.

ESSENTIAL ELEMENTS OF MOLECULAR SPECTROSCOPY

A detailed explanation of the origin of molecular vibrations is beyond the scope of this paper. A sufficient view can be gained by considering the simplest case of all—the diatomic oscillatory. For the diatomic molecule

A-----B

where the masses of atoms **A** and **B** are given by $\mathbf{m_A}$ and $\mathbf{m_B}$, we can assume that the bond between **A** and **B** is a spring with spring constant **k** (analogous to a bond force constant). In the limit where the frequency of oscillation, ν, can be described in the harmonic oscillator approximation, we obtain (from application of simple two body kinematics) the expression

$$\nu = (1 / 2\pi c) (k / m_r)^{1/2}$$

where $\mathbf{m_r}$, the reduced mass of the harmonic oscillator, is given by

$$m_r = (m_A m_B) / (m_A + m_B)$$

The treatment of larger molecules and crystalline lattices is a straightforward extension of this simplified case (see Nakamoto 1986 and Decius and Hexter 1977), and the basic interplay between force constants and atomic masses remains the same, i.e., vibrational frequencies generally increase with increasing bond force constant value and decrease with increasing atomic mass.

Values of ν are usually reported in wavenumbers (cm^{-1}), but occasionally in meV (1 meV = 8 cm^{-1}). The first order (normal mode) vibrational bands of most molecular systems appear between a few tens of cm^{-1} and 4000 cm^{-1}. But for molecules/crystals containing elements other than hydrogen, 2500 cm^{-1} defines the upper end of the frequency range. The characteristic normal mode frequencies of the various forms of carbon, for example, lie between 1000 and 2000 cm^{-1}, whereas, the frequencies of the transition metal oxides and carbides that might be observed for carbon dusting specimens lie below 1000 cm^{-1} (Nakamoto 1986).

From statistical analysis considerations of molecular vibrations, we learn that the populations of vibrational states are governed by Boltzmann statistics, but in almost all instances one is measuring transitions between the ground vibrational state and the first excited state as depicted in Figure 1. Infrared spectroscopy involves the measurement of absorption of discreet quanta of radiation from a white beam of radiation in the infrared portion of the frequency spectrum (10 cm^{-1} to 4000 cm^{-1} for the far- through mid-infrared region). In Figure 1, this would correspond to a transition from state “g” to state “e”. The absorptions occur at frequencies (energies) corresponding to specific vibrational modes of the molecule or crystal being measured.

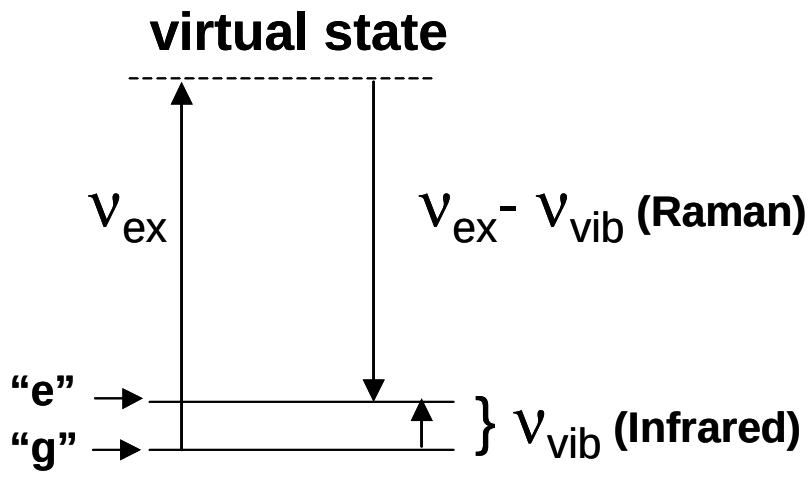

FIGURE 1. Energy Level Diagram for Raman and Infrared Processes

In Raman spectroscopy, one uses a monochromatic excitation source (usually a laser) having a frequency (energy) well above that of the range of typical molecular vibrations/phonons. Lasers with energies that range from 10,000 to 50,000 cm^{-1} can be used, the choice of energy being somewhat dependant on the optical absorption properties of the sample. During Raman scattering, a molecule or crystal absorbs a full quantum of the laser energy (ν_{ex} in Figure 1), rises in energy to a virtual state, and then re-emits the quantum of absorbed laser energy. It will usually re-emit the same quantum of energy (ν_{ex}) and thus return to the original ground state (Rayleigh scattering), but if the molecule undergoes a transition to one of its vibrationally excited states (ν_{vib} in Figure 1) while in the virtual electronic state the emitted quantum of radiation will have an energy $\nu_{ex} - \nu_{vib}$ (Stokes scattering). In the much less likely event that the molecule is in a vibrationally excited state (e.g., state "e" in Figure 1) when it absorbs the quantum of laser energy and returns to the vibrational ground state prior to re-emiting the absorbed laser energy, the emitted radiation will have an energy equal to $\nu_{ex} + \nu_{vib}$ (anti-Stokes scattering). Raman spectroscopy almost always involves the measurement of Stokes scattering.

RAMAN AND INFRARED MODE ACTIVITY AND INTENSITY

The number of degrees of freedom of a molecule or a crystal lattice is equal to three times the number of atoms, **N**, in the molecule or in the unit cell of the crystal. The number of vibrational degrees of freedom for a molecule is determined by subtracting the translational and rotational degrees of freedom (5 for linear and 6 for nonlinear molecules) from 3**N**. For a crystal lattice only the three translational degrees of freedom are subtracted from 3**N**. The number of vibrational degrees of freedom that are observable by either Raman or infrared spectroscopy is determined by analysis of the symmetry properties of the molecule or crystal. The details of such analyses are beyond the scope of this paper, but it is important to note that for isolated molecules, point group symmetry is important (Nakamoto 1986), whereas for crystalline solids, the analysis involves space group algebra (Decius and Hexter 1977 and Fateley et al. 1971). In the case of crystalline solids, the space group symmetry of the crystal lattice and the site symmetries of the individual atoms in the lattice must be known to solve the vibrational secular

equation. Once the number and symmetry type of the vibrational degrees of freedom for a molecule or a crystal have been determined, it is possible to predict the number and symmetry type of the ones that are Raman and/or infrared active. One important aspect of this determination occurs for molecules or crystal lattices that possess a center of inversion. For such molecules or crystals, there will be mutual exclusion of the Raman and infrared active modes, i.e., Raman active modes will be infrared inactive and infrared active modes will be Raman inactive. Part I of Nakamoto (1986) covers all these principals in sufficient detail for most interested readers.

The Raman activity and Raman intensity of a particular normal mode are determined from the polarizability tensors for that mode, whereas infrared activity/intensity are determined from dipole moment tensors. These relationships are shown diagrammatically in Figure 2, where α is the polarizability, μ is the dipole moment, and $\boldsymbol{q}$ is the motional coordinate associated with a particular normal mode. Note that the intensity, **I**, is proportional to $(\boldsymbol{d}\alpha / \boldsymbol{dq})_0$ and $(\boldsymbol{d}\mu / \boldsymbol{dq})_0$ for Raman and infrared activity, respectively. The zero subscript indicates that the derivative is evaluated at the equilibrium (ground state) condition of the motional coordinate. Using the carbon dioxide molecule (a molecule with a center of inversion) as an example, the diagrams in Figure 2 show that the symmetric stretching mode of CO_2 has a non-zero $(\boldsymbol{d}\alpha / \boldsymbol{dq})_0$ but a zero value for $(\boldsymbol{d}\mu / \boldsymbol{dq})_0$, while the antisymmetric stretching mode has a non-zero $(\boldsymbol{d}\mu / \boldsymbol{dq})_0$ but a zero value for $(\boldsymbol{d}\alpha / \boldsymbol{dq})_0$. In the actual spectra of CO_2, the symmetric stretch appears in the Raman spectrum but not in the infrared spectrum, and the antisymmetric stretch appears in the infrared but not the Raman. In a qualitative sense one can see that the polarizability ellipsoids in the stretched and compressed states of the symmetric stretch are not equivalent (in shape and volume), whereas they are for the antisymmetric stretch.

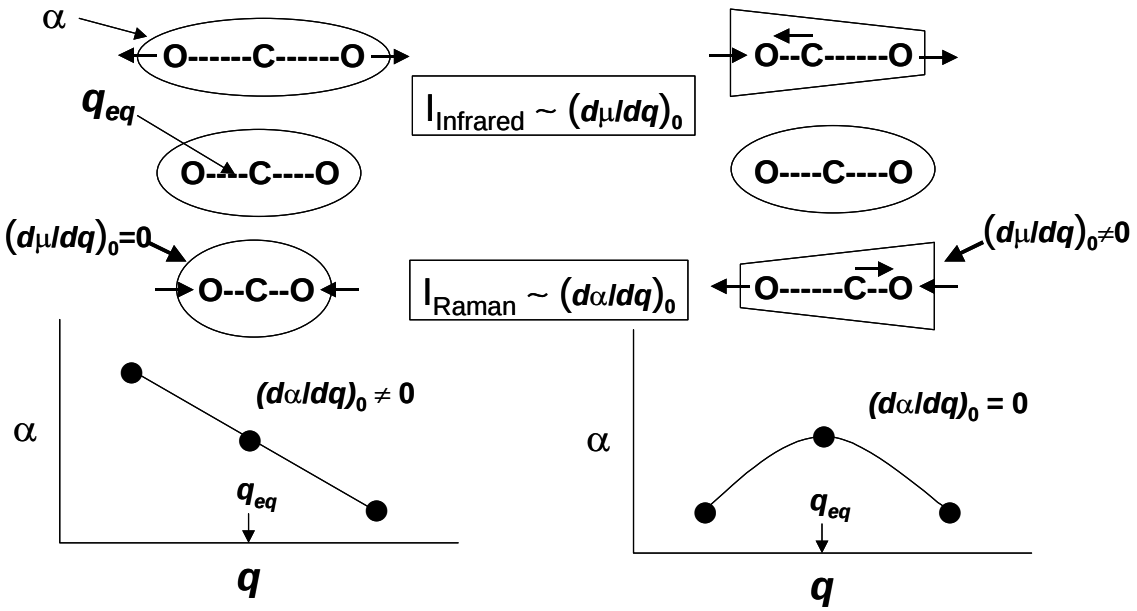

FIGURE 2. Relationship of Symmetry, Dipole Moment (μ), and Polarizability (α) to Raman and Infrared Mode Activity and Intensity

In a crystalline lattice, it is often the case that the lattice contains imperfections. These imperfections can be atomic site vacancies, impurity atoms on lattice sites, misoriented grain boundaries, and interstitial atoms to name a few. Such imperfections destroy the natural symmetry of the perfect crystal and also compromise the selection rules for Raman and infrared activity. If the imperfections prevail over a significant atomic percentage of the lattice, modes that are normally inactive in the Raman or infrared spectrum can become active. As will be shown further on, lattice disorder influences the observed Raman spectra of carbon dusting deposits.

MEASUREMENT OF RAMAN AND INFRARED SPECTRA

Measurement methodologies for Raman and infrared spectra are at a highly developed state. The nature of the basic components for both types of spectroscopies are categorically the same: a source of radiation (monochromatic for Raman, polychromatic for infrared), optics for radiation steering/focusing, a monchromator- or interferometer-based frequency spectrum analyzer (FSA), a detector, and a computer to operate the system and collect/process/store the spectra. While there are still some advantages to dispersive FSAs, most infrared spectroscopy and a fair amount of Raman spectroscopy (particularly on organic materials) are done using instruments that employ interferometric FSAs.

In our experience with the investigation of carbon dusting corrosion, Raman spectroscopy is proving to be more useful than infrared because of the opacity of various forms of carbon to infrared radiation and the relatively strong Raman scattering inherent to most morphological forms of carbon. There are two basic optical configurations for the measurement of laser-induced Raman spectra: the conventional configuration and the microprobe configuration, as diagrammed in Figure 3. In the conventional configuration, the excitation laser is typically brought in at a non-perpendicular angle with respect to the sample surface and the isotropically scattered Raman radiation is collected with a wide-angle optic over an angular range that excludes any specularly reflected laser radiation. In the microprobe configuration, the laser is introduced to the sample through a short focal length lens that also serves as the collection optic. Specially designed optics block backscattered laser radiation so that only the Raman scattering enters the monochromater. The advantage of this configuration is that the short focal length lens can be made part of a microscope, such that the region of the sample being struck by the excitation laser can be viewed and even imaged. With commercially available Raman microprobe instruments, submicron resolution of surface domains on samples is possible (Williams et al. 1996). The Raman results reported in this paper were obtained using a Renishaw System 2000 Imaging Raman Microscope equipped with a He-Ne laser (633 nm).

RAMAN MICROSCOPY OF CARBON DUSTING SPECIMENS

An extensive series of Raman measurements on loose carbon dusts and on metal coupons from carbon dusting experiments has been made at the Argonne National Laboratory over then past year. Selected examples of the types of results obtained in these measurements will be presented in this section. Additional descriptions of the results and their implications with respect to the mechanism(s) of carbon dusting are presented in a companion publication (Zeng et al. 2002). It has turned out in these measurements that informative spectral features can be found over a wide frequency range (200 to 3400 cm^{-1}).

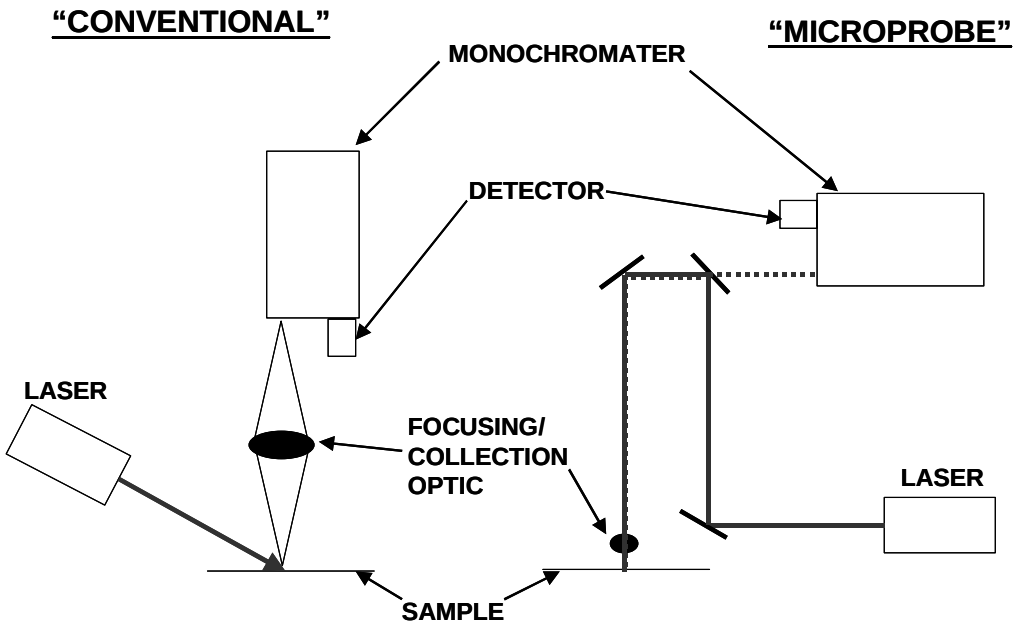

FIGURE 3. Schematic Layouts for "Conventional" and "Microprobe" Type Raman Spectroscopy Measurements

Raman spectra of carbon dust from experiments wherein iron coupons were subjected to two different dusting environments are shown in Figures 4 through 6; the test conditions are tabulated in Table 1. In these experiments the exposure environment was flowing gaseous CO + H_2 + CO_2 and the exposure conditions were 100 hours at 1300°F for Tests 4 and 5 and 5 hours at 1100°F for Test 7. The difference between Test 4 and Test 5 was that H_2O was also present in the gas mix in the case of Test 5. Let us first consider the spectra in the 200 to 1000 cm^{-1} region (Figure 4). There are no Raman bands in this spectral region for the dusts from the longer-duration/higher-temperature exposure tests (the spectrum labeled Test 4&5 in Figure 4 is representative of all such exposures). This is also the case for the Raman spectra of the two types of graphite included in Figure 4 and is consistent with expectation for graphitic carbons (Knight and White 1989). The bands that appear with varying intensity in the Raman spectra of two samples of the dust from Test 7 (the spectra labeled Test 7 and Test 7a in Figure 4) are due to iron oxide particles commingled with the carbon dust. This observation will be discussed in more detail further on.

TABLE 1. Conditions for Carbon Dusting Tests

Test No.	Test Atmosphere	Temperature (°F)	Time (hours)
3	CO + H_2 + CO_2 + H_2O	1100	5
4	CO + H_2 + CO_2	1300	100
5	CO + H_2 + CO_2 + H_2O	1300	100
6	CO + H_2 + CO_2 + H_2O	1100	5
7	CO + H_2 + CO_2	1100	5

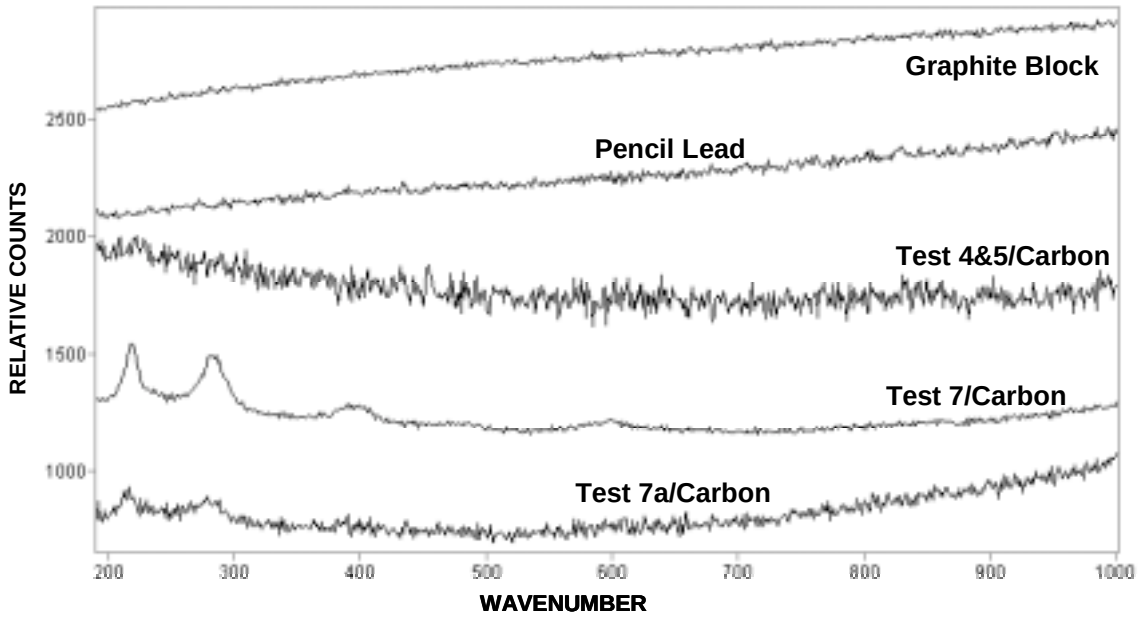

FIGURE 4. Raman Spectra (200-1000 cm^{-1}) of Commercial Graphite, Pencil Lead, and Specimens of Carbon Particles from Carbon Dusting Corrosion Tests

Raman spectra of the same set of samples in the 1000 to 2000 cm^{-1} are shown in Figure 5. This spectral region contains the characteristic first order phonons of all forms of carbon. The spectra of the two graphite samples are typical of medium- to high-density graphitic materials. The mode nominally at 1580 cm^{-1} is the Raman active E_{2g} phonon of graphite (Knight and White 1989). The other prominent band at ca. 1360 cm^{-1} is due to a mode of graphite that would be inactive in a perfect (defect free) graphite crystal and will hereinafter be referred to as the D band per the nomenclature of Mernagh et al. (1984). Its appearance and intensity relative to the 1580 cm^{-1} band is a measure of the extent of disorder in the graphitic material (Lespade et al. 1982). The appearance of the 1360 cm^{-1} band is often accompanied by the observation of a shoulder on the high frequency side of the E_{2g} phonon (ca. 1620 cm^{-1}) as noted by Nakamizo et al. (1978). The graphite block and the pencil lead exhibit all three of these spectral features to some extent (Figure 5), as do most commercially available forms of graphite (Nakamizo et al. 1974); but the carbon dusts from Tests 4, 5, and 7 showed even greater amounts of disorder. The lower test temperature (1100°F) and shorter exposure time (5 hours) of Test 7 produced a slightly more disordered carbon dust in a CO + H_2 + CO_2 atmosphere than did the higher-temperature (1300°F)/longer-term (100 hours) conditions of Test 4. The addition of water to the sweep gas mix (Test 5) appeared to reduce the disorder level in the dust relative to the result for Test 4.

Raman spectra in the 2000 to 4000 cm^{-1} region for this same series of samples (see Figure 6) contain mainly broad weak bands that are attributed to the overtones and combinations of the D and E_{2g} modes (i.e., 2D, D+E_{2g}, and 2 E_{2g}) per Sato et al. (1978). The most intense feature in this spectral region is 2D, but the factor(s) influencing the variations of its relative intensity in the case of the liberated carbon particles from these particular carbon-dusting experiments needs further investigation.

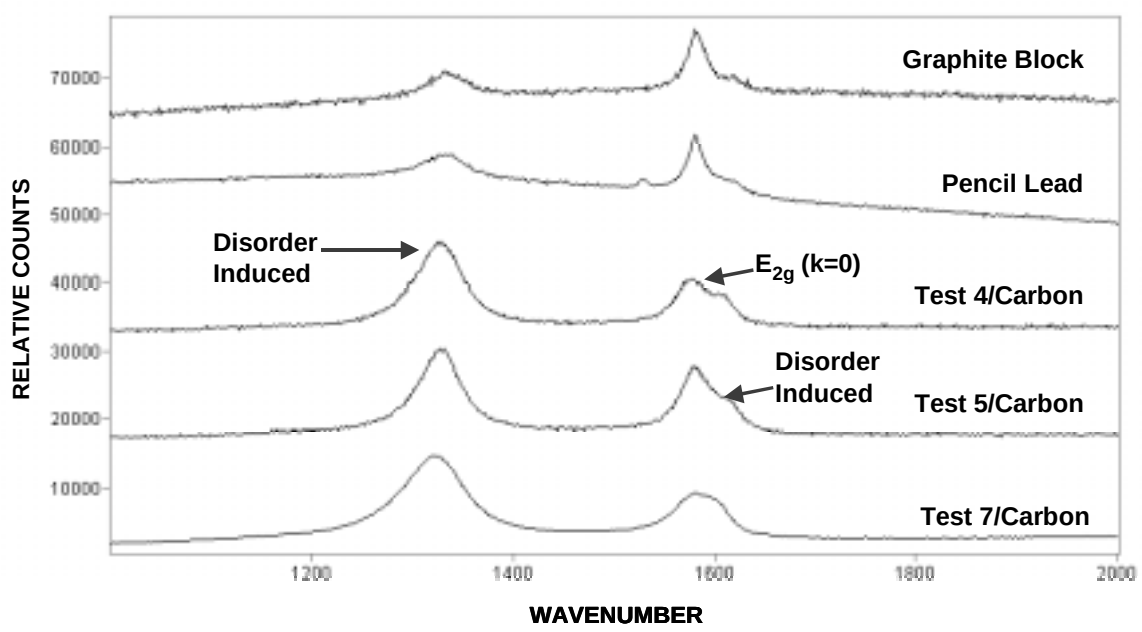

FIGURE 5. Raman Spectra (1000-2000 cm^{-1}) of Commercial Graphite, Pencil Lead, and Specimens of Carbon Particles from Carbon Dusting Corrosion Tests

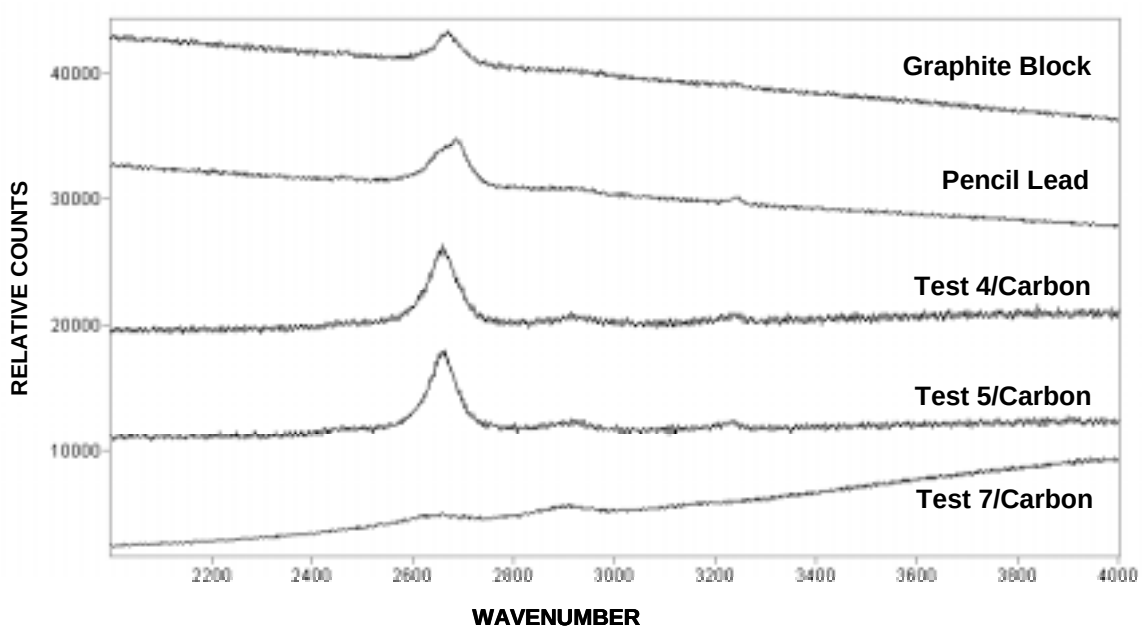

FIGURE 6. Raman Spectra (2000-4000 cm^{-1}) of Commercial Graphite, Pencil Lead, and Specimens of Carbon Particles from Carbon Dusting Corrosion Tests

Now let us consider the results of Raman microprobe examinations of the surfaces of the iron coupons from the tests listed in Table 1. As the results for the 200 to 1000 cm^{-1} region (Figure 7) show, the spectra of specimens from the 1100°F/five-hour exposures (Tests 3, 6, and 7) all contain the Raman active phonons of Fe_2O_3 (Thibeau et al. 1978). Note (1) that the Fe_2O_3 phonons are more intense for the tests with H_2O in the exposure atmosphere and (2) that they do not appear on the surface of specimens exposed for 100 hours at 1300°F (Test 4 and Test 5), whether or not H_2O was present in the exposure atmosphere. In the 1000 to 2000 cm^{-1} region (Figure 8), we observe the D and E_{2g} phonons in an intensity ratio that gives evidence of a highly disordered surface-bound graphite. And again, as was seen in Figure 5, the carbon dust produced at the lower-temperature/shorter-time conditions exhibits the greatest disorder. The 2D, D+E_{2g}, and 2 E_{2g} overtone and combination bands for the residual carbon on the specimen surfaces are more pronounced (Figure 9) than for the dusts (i.e., Figure 6) but the relative intensities for the different exposure conditions appear to be the same.

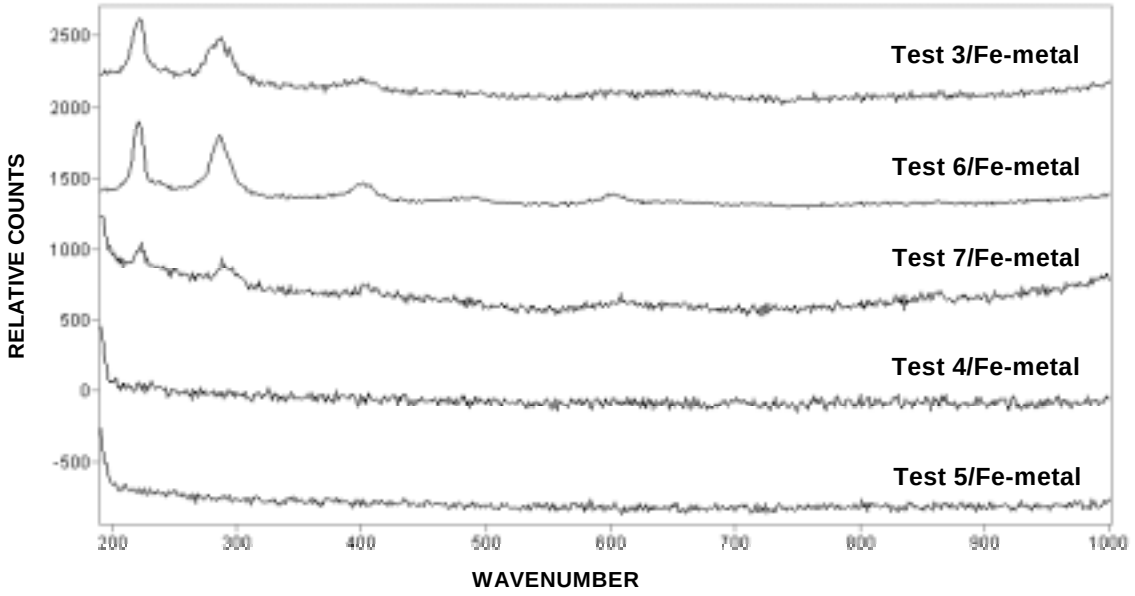

FIGURE 7. Raman Spectra (200-1000 cm^{-1}) of the Surface of Iron Specimens from Carbon Dusting Corrosion Tests

The results in Figures 4 through 9 illustrate the type of information that can be gained from the study of carbon dusting using Raman spectroscopy methods. For example, we find that the carbon dusting of iron exhibits a measurable sensitivity to exposure conditions. Five hours at 1100°F in a flowing CO + H_2 + CO_2 atmosphere produces as much dusting as 100 hours at 1300°F in the same atmosphere; but the lower temperature seems to induce the formation of Fe_2O_3 which dislodges from the iron surface and mingles with the loose carbon dust. The presence of H_2O in the sweep gas enhances the formation of Fe_2O_3. The relative intensities and full-width at half-maximum (FWHM) of the D and E_{2g} modes for the surface-bound carbon (and the loose dust as well) reveal that the 1100°F exposure conditions produce a more disordered graphitic dust than the 1300°F conditions. It is most likely the case that the dust formed at lower temperature has a smaller average particle size (Lespade et al. 1982). Manifestations of the effect of the presence of H_2O on the spectral features of the graphitic carbon phonons are not as obvious—the most critical factor appears to be temperature.

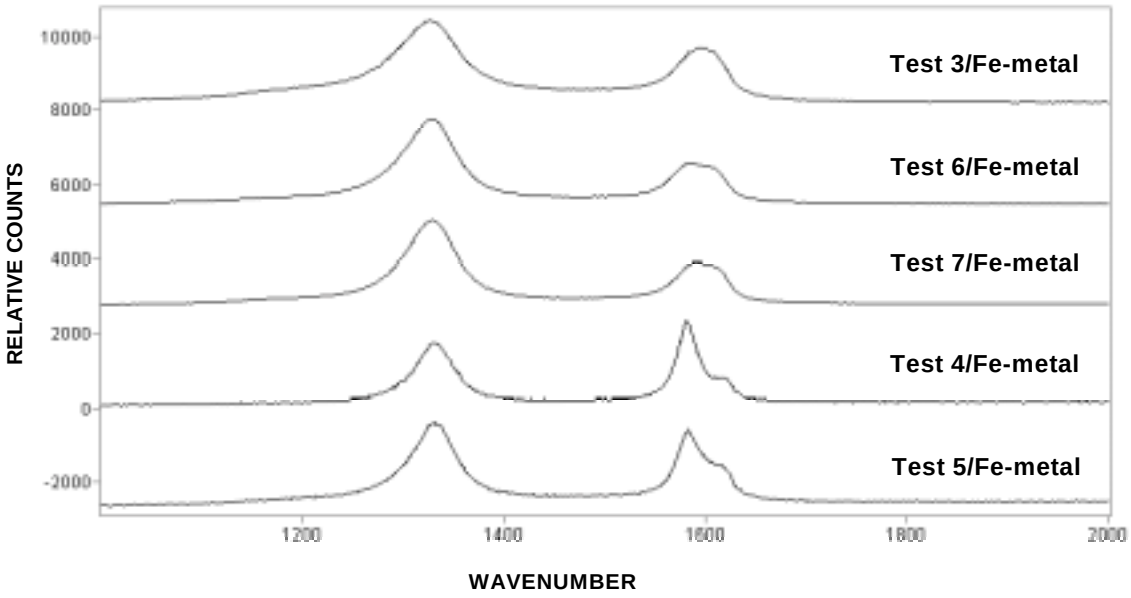

FIGURE 8. Raman Spectra (1000-2000 cm^{-1}) of the Surface of Iron Specimens from Carbon Dusting Corrosion Tests

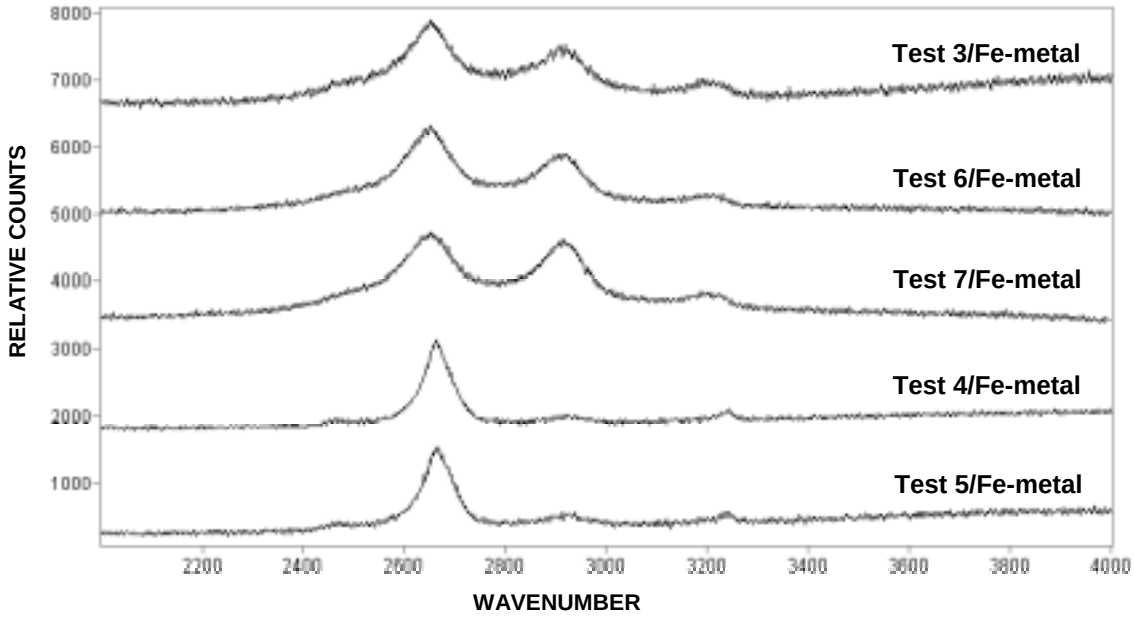

FIGURE 9. Raman Spectra (2000-4000 cm^{-1}) of the Surface of Iron Specimens from Carbon Dusting Corrosion Tests

Our collective interpretation of these results is that the dominant factor affecting the Raman observations for the carbon dusts (both the liberated dusts and the surface-bound carbon) is the graphite grain size. Using the work of Lespade et al. (1982) as a guide, we would conclude from Figures 4 and 7 that the grain size is <10 nm for the higher temperature exposures and <5 nm for

the lower temperature exposures. With such small grain sizes, it is not surprising that the D band and the 1620 cm^{-1} band (sometimes referred to as the D′ band) appear with considerable intensity. These bands arise from the loss of local inversion symmetry experienced by the carbon atoms near grain boundaries, the preponderance of surface carbon atoms, and quite possibly randomization of the ordering of successive carbon layers (turbostatic stacking) as discussed by Knight and White (1989). The appearance of Fe_2O_3 commingled with the liberated carbon dust is surely an indicator and a manifestation of the erosive nature of carbon dusting. The reader is referred to the companion paper by Zeng et al. (2002) for a fuller discussion of the mechanistic aspects of carbon dusting in relation to the experiments described in this paper.

PERSPECTIVE ON FUTURE MOLECULAR SPECTROSCOPY STUDIES OF CARBON DUSTING CORROSION

The next logical step in such studies is to perform the Raman and infrared measurements in situ. In the case of Raman measurements, this would probably have to be done using the conventional methodology diagrammed in Figure 3. Because of the likely need to have the collection optic close to the specimen surface, applications of the microprobe method will require the use of an optical element that can withstand the exposure conditions (particularly the temperature). The possibility for developing such optics is currently under investigation in our laboratory as is the in situ study of carbon dusting using conventional Raman microscopy.

Infrared spectroscopy can be used in at least two ways for the study of metal dusting. One is to use transmission methods to monitor the gas phase species during carbon dusting. This could be done in the elevated temperature environment with a fiber-optically-coupled immersion probe or in a specially designed cell outfitted with multi-pass infrared optics; but it could also be done downstream of the exposure zone using a flow-through gas cell. Most vendors of infrared sampling accessories provide products that are suitable for these types of measurements.

For direct in situ measurements of metal dusting corrosion we are looking into the possible application of diffuse reflectance infrared Fourier transform (DRIFT) methods. The type of accessory we have used successfully in the past to obtain real-time in situ infrared spectra of solid samples in flowing-gas environments at elevated temperature is shown in Figure 10. The operational details for this accessory (as used in our work) have been described in papers by Johnson et al. (1988) and Maroni and Epperson (2001). In brief, process gas introduced at the *gas entrance port* flows upwards along the cal-rod-heated *sample post*. The heated process gas passes over the sample resting atop the *sample post* inside the *sample cup*, into a labyrinth at the base of the *sample cup*, and out of the cell via the *gas exit port*. The infrared beam is focused onto the sample by an external parabolic mirror and the diffuse scattering is collected with a second external parabolic mirror. The focused incoming beam and the diffuse scattering pass through the *windows* in the dome above the *sample cup*. In past work with this cell we were able to record interpretable DRIFT spectra of samples at temperatures as high as 1100°F. It should be possible to conduct carbon dusting experiments comparable to Tests 3, 6, and 7 in Table 1 using this cell.

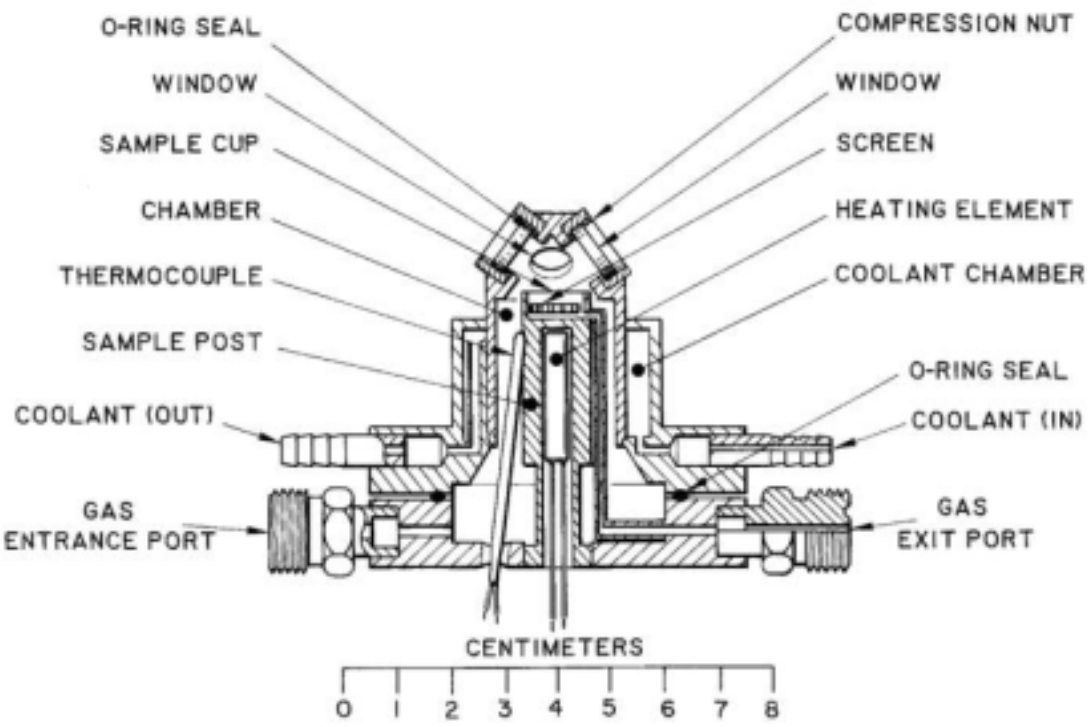

FIGURE 10. Controlled Environment Diffuse Reflectance Cell

Another potentially useful infrared technique that may be applicable to the study of carbon dusting corrosion is attenuated total reflection (ATR) spectroscopy. An ATR-based approach that has been used successfully to study particulate matter is diagrammed in Figure 11. In this approach, particulate matter in a flowing gas stream is size segregated using a nozzle-type particle impactor. Particles of a specific size range are impacted onto ATR plates. By stacking the ATR plates and moving them through the nozzle gap, it is possible to study the evolution of the particulate matter as a function of time. The integration of the ATR approach into an instrument with a built in FTIR measurement capability has been done in our laboratory. This device, called the infrared aerosol analyzer (IAA), has been used to study the chemistry of atmospheric particulate matter (Johnson et al. 1983, Novick et al. 1999). Its adaptation to the study of carbon particles in the gaseous environments downstream of carbon dusting exposures should be straightforward. Specifically, in addition to observing the infrared active phonons of the various chemical and morphological forms of carbon that are created during dusting, it should be possible to detect molecular species adsorbed on the carbon particles.

Finally, it is noteworthy in closing to mention that in the field of materials science, molecular spectroscopy results often couple very informatively with the results of other types of analytical measurements, such as electron microscopy and x-ray diffraction, as well as with measurement methods that probe surface area, particle size distributions, and stress/strain fields.

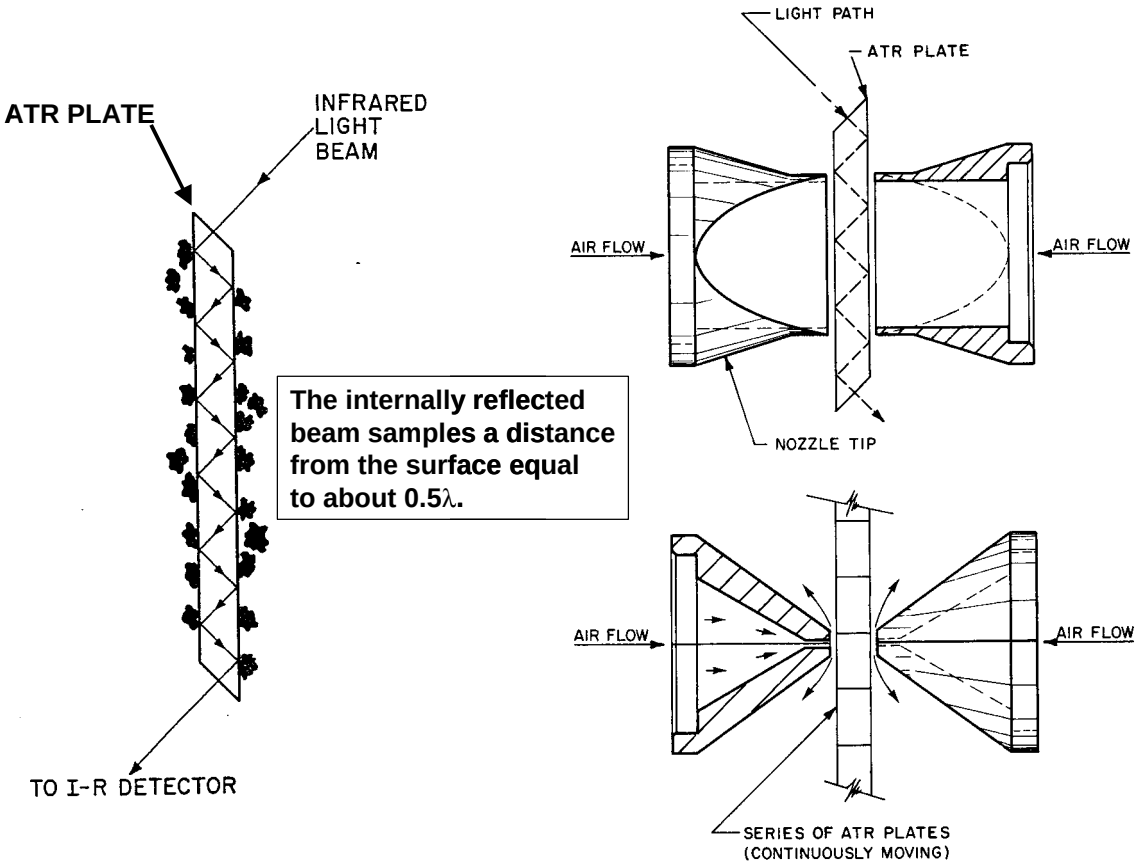

FIGURE 11. Features of the ATR Impactor Method for Investigating the Infrared Spectra of Fine Particles in Gas Streams

ACKNOWLEDGEMENT

This research was sponsored by the Office of Industrial Technologies, U.S. Department of Energy under Contract W-31-109-ENG-38.

REFERENCES

1. Decius J.C., and R.M. Hexter, 1977, *Molecular Vibrations in Crystals*, McGraw-Hill.

2. Fateley, W.G., N.T. McDevitt, and F.F. Bently, 1971, "Infrared and Raman Selection Rules for Lattice Vibrations," *Applied Spectroscopy* 25:155-173.

3. Ferraro, J.R., and K. Krishnan, 1990, *Practical Fourier Transform Infrared Spectroscopy*, Academic Press

4. Johnson, S.A., R. Kumar, and P.T. Cunningham, 1983, "Airborne Detection of Acidic Sulfate Aerosol Using an ATR Impactor," *Aerosol Sci. Technol.* 2:401

5. Johnson, S.A., R.-M. Rinkus, T.C. Diebold, and V.A. Maroni, 1988, "The Use of Diffuse Reflectance Infrared Spectroscopy for Studies of Molecular Sieve Catalysis," *Applied Spectroscopy* 42:1369-1375.

6. Knight, D.S., and W.B. White, 1989, "Characterization of Diamond Films by Raman Spectroscopy," *Journal of Materials Research* 4:385-393.

7. Lespade, P., R. Al-Jishi, and M.S. Dresselhaus, 1982, "Model for Raman Scattering from Incompletely Graphitized Carbons," *Carbon* 20:427-431.

8. Maroni, V.A., and S.J. Epperson, 2001, "An In Situ Spectroscopic Investigation of the Pyrolysis of Ethylene Glycol Encapsulated in Silica Sodalite," *Vibrational Spectroscopy* 27:43-51.

9. Mernagh, T.P., R.P. Cooney, and R.A. Johnson, 1984, "Raman Spectra of Graphon Carbon Black," *Carbon* 22:39-42.

10. Nakamizo, M., H. Honda, and M. Inagaki, 1978, "Raman Spectra of Ground Natural Graphite," *Carbon* 16:281-283.

11. Nakamizo, M., R. Kammereck, and P.L. Walker, Jr., 1974, "Laser Raman Studies of Carbons," *Carbon* 12:259-267

12. Nakamoto, K., 1986, *Infrared and Raman Spectra of Inorganic and Coordination Compounds*, 4th Edition, John Wiley & Sons.

13. Novick, V.J., S.A. Johnson, H.A. Hisgen, and V.J. Reyes, 1999, "Real Time Chemical Vapor Detection and Enhancement Utilizing Aerosol Adsorption," *Rev. Sci. Instrumen.* 70:1829

14. Sato, Y, M. Kamo, and N. Sekata, 1978, "Raman Spectra of Carbons at 2600-3300 cm^{-1} Region," *Carbon* 16:279-280.

15. Suëtaka, W., 1995, *Surface Infrared and Raman Spectroscopy: Methods and Applications*, Plenum Press.

16. Thibeau, D., C.W. Brown, and R.H. Heidersbach, 1978, "Raman Spectra of Possible Corrosion Products of Iron," *Applied Spectroscopy* 32:532-535.

17. Williams, K.P.J., I.C. Wilcock, I.P. Hayward, and A. Whitely, 1996, "Applications of State-of-the-Art Raman Microscopy and Direct Raman Imaging," *Spectroscopy* 11:45-50.

18. Zeng, Z., K. Natasan, and V.A. Maroni, 2002, "Study of Metal Dusting Mechanism in Iron Using Raman Spectroscopy and X-Ray Diffraction," pp.???-??? in *The Proceedings of the International Workshop on Metal Dusting*, September 26-28, 2001, Argonne National Laboratory, Argonne, IL.